Coherent internal and centre of mass quantum rotation of methyl groups in the ***p***-tert-butyl-calix[4]arene(2:1) ***p***-xylene supramolecular complex

1998 J. Phys.: Condens. Matter 10 2221

(http://iopscience.iop.org/0953-8984/10/10/006)

J. Phys.: Condens. Matter **10** (1998) 2221–2231. Printed in the UK PII: S0953-8984(98)86622-8

Coherent internal and centre of mass quantum rotation of methyl groups in the *p*-tert-butyl-calix[4]arene(2:1)*p*-xylene supramolecular complex

P Schiebel†, G Amoretti‡, C Ferrero§, B Paci‖, M Prager¶ and R Caciuffo‖

† Institut Laue–Langevin, Boîte Postale 156, F-38042 Grenoble Cédex 9, France, and Institut für Kristallographie, Universität Tübingen, D72070 Tübingen, Germany

‡ Dipartimento di Fisica, Università di Parma, Viale delle Scienze, I-43100 Parma, and Istituto Nazionale per la Fisica della Materia, Unità di Parma, Italy

§ European Synchrotron Radiation Facility, Boîte Postale 220, F-38043 Grenoble Cédex, France

‖ Dipartimento di Scienze dei Materiali e della Terra, Università di Ancona, and Istituto Nazionale per la Fisica della Materia, Unità di Ancona, Via Brecce Bianche, I-60131 Ancona, Italy

¶ Institut für Festkörperforschung des Forschungszentrum, D-52425 Jülich, Germany

Received 4 August 1997, in final form 11 November 1997

Abstract. The low-temperature inelastic neutron scattering spectrum measured for the *p*-tert-butylcalix[4]arene(2:1)*p*-xylene complex has been interpreted in the framework of a quantum dynamical model assuming a rotational motion of the *p*-xylene CH_3 groups correlated to the translational motion of their centre of mass. By comparing the experimental data with calculated energies and intensities, the effective anharmonic and anisotropic molecular potential experienced by the methyl groups has been derived. The wavefunctions deduced from the spectroscopy results are used to calculate the proton density distribution in the plane of the motion.

1. Introduction

Inelastic neutron scattering (INS) spectroscopy has been widely used in the past twenty years to study single-particle rotations in molecular crystals, giving a wealth of useful information on the correlations between the macroscopic properties of a molecular solid and the orientational freedom of its constituents [1, 2]. A large number of systems has been investigated in which the rotating groups experience a relatively strong barrier to reorientation. In these cases, the low-temperature dynamics can be described in terms of torsional excitations, taking into account that the degeneracy of the torsional levels is lifted by tunnelling between different potential minima. The tunnelling splitting is very sensitive to the barrier height, decreasing rapidly as the barrier height increases. Therefore, its experimental determination generally allows an accurate estimation of the symmetry and magnitude of the potential energy surface, which is in turn strongly dependent on the molecular conformation in the solid and on the nature of the binding forces.

A more subtle behaviour is found in those molecular crystals where the hindering potential is so weak that the limit of quantum-mechanical free rotation is approached. The rotational dynamics become indeed very sensitive to the details of the motion, and the isolated single-particle model usually fails to correctly describe the experimental evidence. Almost free rotations have been observed in several solid state systems containing molecules

0953-8984/98/102221+11$19.50

with one or more NH_3 or CH_3 groups, such as toluene, nitromethane, γ-picoline [3–5], and several calixarene supramolecular complexes [6, 7]. The failure of the single-particle model in explaining the experimental spectra recorded for these systems has stimulated alternative interpretations, based on the assumption of different kinds of coupling between rotors or between the rotors and the environment [8–10]. However, when experimental results and theoretical predictions are compared, the attention is usually limited to the energy at which the various excitation lines occur, irrespectively of their intensities. In other words, the agreement with the experiment is judged only on the basis of the eigenvalues of the model Hamiltonian. Now, as discussed in [7], this procedure is quite ambiguous, because it is often possible to fit the position of the lines in a spectrum with more than one set of parameters of a given Hamiltonian, or even with different Hamiltonians, corresponding to significatively different physical situations. A more satisfactory approach is to try and reproduce also the relative intensities of the observed excitations, in order to test the eigenfunctions of the model Hamiltonian, as well as its eigenvalues. The reason why this has been done only in the framework of the single-particle model of rotational dynamics is that intensity calculations are generally quite cumbersome.

In a previous experiment we used INS measurements to study the internal rotational dynamics of the *p*-xylene methyl groups in a fully protonated sample of *p-tert*-butylcalix[4]arene(2:1)*p*-xylene [10]. At a temperature $T = 2$ K, several inelastic peaks were observed, at 0.626(1), 1.62(1), 1.85(1), 2.20(1) and 2.48(1) meV. The peak at 2.20 meV has a larger width than the others but, in spite of this, in [10] it was assumed to correspond to a single excitation. An increase of the temperature from 2 to 25 K was accompanied by a shift of the most intense line from 0.627 meV up to 0.660(6) meV. It must be noticed that 0.660(6) meV is an energy higher than the free rotor limit for the CH_3 group, i.e. 0.647 meV. The observed excitations were interpreted in [10] as transitions between tunnel-split librational states of the *p*-xylene methyl groups, assuming a coupling between the rotational motion of the CH_3 and the librations of the whole *p*-xylene molecule. The peaks at 1.62 and 2.20 meV were attributed to cross-transitions involving simultaneous excitations or de-excitations of both methyl rotational levels and librational levels of the *p*-xylene. With this model it was possible to obtain a very good agreement between the observed excitation *energies* and the values calculated from the spectrum of the Hamiltonian

$$H = -B_M \frac{\partial^2}{\partial \phi_1^2} - B_X \frac{\partial^2}{\partial \phi_2^2} + \frac{1}{2} V_6 \{1 - \cos(6\phi_1)\} + V_4 \phi_2^2 \tag{1}$$

with a sixfold methyl rotational barrier of height $V_6 = 6.5$ meV, and a four-fold librational potential $V_4 = 13.8$ meV ($B_M = 0.647$ meV and $B_X = 0.022$ meV are the rotational constant for the methyl and the *p*-xylene molecule, respectively).

To verify the predictions of this model, we repeated the experiment with a sample containing partially deuterated *p*-xylene (CH_3–C_6D_4–CH_3), expecting a shift towards lower energies of the peaks at 1.62 and 2.20 meV (due to the increased momentum of inertia) and a reduction of their intensities (because of the different neutron cross-section for H and D isotopes). However, much to our disappointment, the experimental spectra obtained for the partially deuterated sample and for the fully protonated one do not show significative differences. Thus, the model described in [10] fails.

In this paper, we give an alternative interpretation of the high-resolution INS cross section measured at low temperature for the *p-tert*-butylcalix[4]arene(2:1)*p*-xylene supramolecular complex. By comparing theoretical predictions with *energy and intensity*

of the observed excitations, we suggest that the motion of the protons in the CH_3 groups of the *p*-xylene molecule corresponds to a hypocycloidal classical orbit, resulting from a synchronous reverse rotation of the methyl groups and of their centre of mass.

2. Experimental details and results

Calix[*n*]arenes are bowl-shaped synthetic macrocycles with ordered arrays of H-bonded phenol–methylene oligomers [11]. The number of the phenolic units can vary from $n = 4$ to $n = 14$, and different substituents can be attached to the aromatic ring in the *para* position and at the phenolic oxygen. The most interesting property of calixarenes is their ability to incarcerate neutral and ionic guests in supramolecular three-dimensional arrays. For this reason, they have attracted much attention, in the past few years, as molecular receptors for selective ion complexation.

At room temperature, the *p-tert*-butylcalix[4]arene(2:1)*p*-xylene complex crystallizes in the tetragonal $P4/n$ space group, with lattice parameters $a = 12.823(5)$ Å and $c = 25.618(6)$ Å [12]. The guest *p*-xylene molecule is held in a closed cavity formed by two calixarene units facing their *tert*-butyl groups. A side view of the molecular cage, including the guest, is shown in figure 1. The complex lies on a crystallographic fourfold axis running along the CH_3–C_{ph} bond of the *p*-xylene.

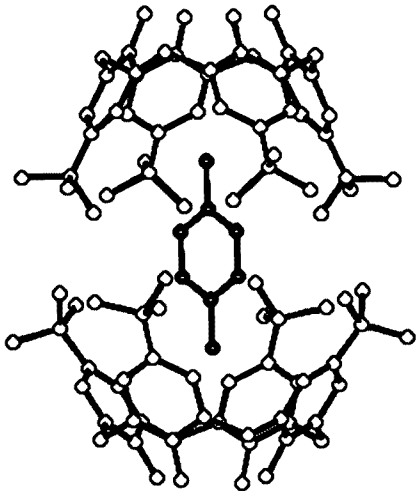

Figure 1. Molecular conformation of the *p-tert*-butylcalix[4]arene(2:1)*p*-xylene complex. Side view perpendicular to the fourfold axis. Protons are not shown.

A sample of about 2 g, containing partially deuterated *p*-xylene (CH_3–C_6D_4–CH_3, 98% atom D in the phenyl ring, as determined from NMR measurements), was prepared at the University of Parma and shown to be single phase by x-ray diffraction. High-resolution INS measurements were performed with the time-of-flight inverted-geometry crystal analyser spectrometer IRIS, at the ISIS spallation neutron source of the Rutherford Appleton Laboratory, Oxfordshire, UK. The spectrometer was operated with (002) pyrolitic graphite analysers close to back-scattering, using 51 separate detector angles, between 20 and 160 degrees. The energy transfer varied from -0.7 to 2.6 meV, with a resolution of about 15 μeV at the elastic peak. The sample was mounted into a flat aluminium can inside

a standard He cryostat and the INS spectra were recorded at different temperatures varying from 4.2 to 40 K.

The results of the measurements are practically the same as those obtained for the fully protonated sample and reported in [10]. The neutron intensity distribution obtained at 4.2 K is shown as an example in figure 2. In particular, the substitution of deuterium for hydrogen in the aromatic ring of the *p*-xylene does not modify energy and intensity of the neutron groups at 1.62 and 2.20 meV which, following the interpretation given in [10], were associated to librational excitations of the whole *p*-xylene. However, the IRIS data clearly show that the group at 2.20 meV is split into two peaks. By fitting each peak to the instrument lineshape we find excitation energies of 0.626(1), 1.603(5), 1.849(5), 2.10(1), 2.21(1) and 2.48(1) meV, with a further very small line at 1.24(2) meV. Of the two peaks which are visible immediately above 1.6 meV, the one at 1.603 meV is a true transition, whilst the line at 1.65 meV is a spurious signal originating from the (004) Bragg reflection of the pyrolitic graphite crystal analysers. This can be verified by examining separately the time-of-flight spectra of the different detectors, and is confirmed by the INS distribution obtained with the multichopper spectrometer MIBEMOL, at the Laboratoire Léon Brillouin, France (inset of figure 2). The small bump around 0.9 meV has the same origin. As shown in figure 3, a weak line can be identified at 2.73(3) meV; it must be noticed that this energy falls at the end of the accessible range where the data are less reliable because of the large values of the Jacobian for the time-of-flight to energy conversion. The spin temperature derived from the intensity ratio of the energy-gain to the energy-loss lines at 0.626 meV is $T_S = 26$ K.

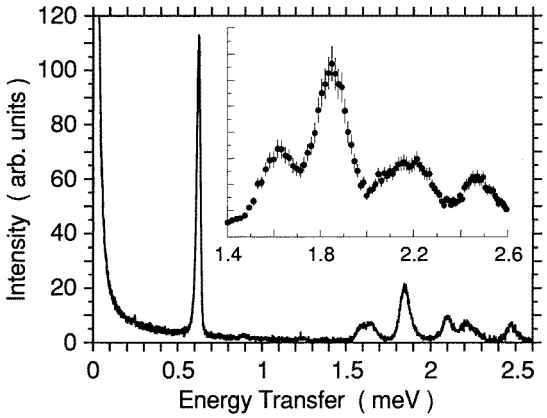

Figure 2. INS spectrum of the (2:1) complex of CH_3–C_6D_4–CH_3 with *p-tert*-butylcalix[4]arene, measured between 0 and 2.6 meV with the IRIS spectrometer ($T = 4.2$ K). The inset shows the spectrum of the same sample recorded with the MIBEMOL spectrometer.

A similar study on a calixarene complex with toluene as a guest shows that no peaks are visible in the INS spectra of the empty cage [13]. Therefore, we must conclude that all the peaks in the cross-section shown in figure 2 are linked to the dynamics of the *p*-xylene CH_3 groups only. The model outlined in [10] must be discarded not only because we do not observe the isotopic effects which should be involved by a librational motion of the *p*-xylene molecule, but also because the extra splitting revealed around 2.20 meV cannot be fitted in the energy level scheme of [10], the number of possible transitions being too small to account for all the observed peaks.

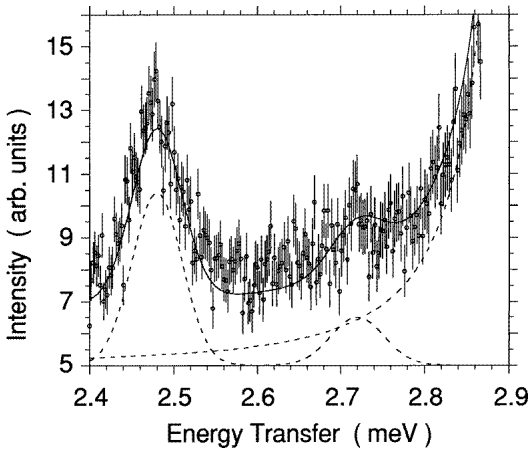

Figure 3. INS spectrum at 4.2 K between 2.4 and 2.9 meV (IRIS spectrometer). Full line: averaged spectrum; dotted line: after background subtraction.

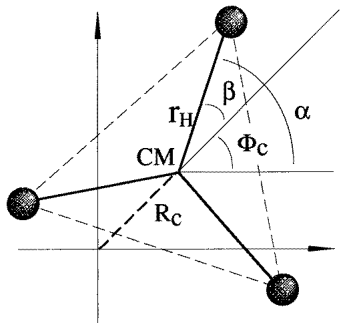

Figure 4. Definition of the coordinate system used to describe the motion of the CH_3 protons and of their centre of mass (CM).

3. Rotation–translation coupling model

A consistent description of the experimental results can be given by assuming that the uniaxial rotation of the methyl group is accompanied by a translation of its centre of mass (CM) along a closed loop in the plane defined by the three protons. The corresponding classical motion would be a synchronous reverse rotation of the CM around the fourfold axis of the calixarene cage, and of the proton triangle about the CM. This is the same model as used by Schiebel *et al* [14] to reproduce the proton density distribution obtained by neutron diffraction in nickelhexammine salts, where NH_3 molecules rotate around a crystallographic site with fourfold symmetry, and by Havighorst and Prager [15] to interpret the ammonia tunnelling in Hofmann clathrates. The reference frame used to describe the proton dynamics is shown in figure 4. If the methyl triangle is considered to be rigid and equilateral, a given setting of the CH_3 group is uniquely defined by the polar coordinates of CM (R_c, Φ_c), and by the angle $\alpha = (\beta + \Phi_c)$ associated with the rotation around CM. The C–H bond length is assumed to be $r_H = 1.037$ Å.

The symmetry-adapted crystal potential experienced by each proton [14] is given by a linear combination of spherical harmonics as:

$$V_C(r_i, \phi_i) = \tfrac{1}{2} A r_i^2 + \tfrac{1}{4} B r_i^4 \cos(4\phi_i) + \tfrac{1}{4} C r_i^4 \tag{2}$$

where A, B and C are three parameters to be determined, and $(r_i,\ \phi_i)$ are the polar coordinates for the ith proton. The effective molecular potential for the CH_3 group in a given setting is then obtained by summing the terms acting on each of the protons:

$$V_M(R_c, \Phi_c, \alpha) = \sum_{i=1}^{3} V_C(r_i, \phi_i) = 3(V_M^0 + V_M^R + V_M^W) \tag{3}$$

where V_M^0 is an irrelevant constant term,

$$V_M^R(R_c) = \left(\frac{A}{2} + C r_H^2\right) R_c^2 + \frac{1}{4} C R_c^4 \tag{4}$$

is the average of the potential over the angular variables and

$$V_M^W(R_c, \Phi_c, \alpha) = B r_H^3 R_c \cos(\Phi_c + 3\alpha) + \tfrac{1}{4} B R_c^4 \cos(4\Phi_c) \tag{5}$$

is the term allowing for the coupling between the position of the CM (R_c, Φ_c) and the orientation of the methyl triangle (α).

The Schrödinger equation for the two-dimensional motion of the CM, coupled to the uniaxial rotation of the methyl, is then

$$\left(\frac{\boldsymbol{P}_c^2}{2M} + B_M L^2 + V_M(R_c, \Phi_c, \alpha)\right) |\psi\rangle = E|\psi\rangle \tag{6}$$

where $\boldsymbol{P}_c$ is the momentum operator for the translational motion of the CM, L is the angular momentum for the uniaxial rotation and $M = 15$ au is the methyl mass. The wavefunction $\psi_j = \langle R_c \Phi_c \alpha | \psi_j \rangle$ associated with a given eigenvalue $\hbar\omega = E_j$ can be expanded in the basis of the eigenstates $|nm\ell\rangle$ of the unperturbed Hamiltonian ($V_M = a R_c^2$), that is into products of 2D harmonic oscillator and 1D rotator wavefunctions,

$$\langle R_c \Phi_c \alpha | \psi_j \rangle = \sum_{nm\ell} a_{nm\ell}^j \langle R_c \Phi_c \alpha | nm\ell \rangle \tag{7}$$

where

$$\langle R_c \Phi_c \alpha | nm\ell \rangle = \frac{1}{2\pi} \hat{R}_n^{|m|}\, \mathrm{e}^{\mathrm{i}m\Phi_c}\, \mathrm{e}^{\mathrm{i}\ell\alpha} \tag{8}$$

with the radial part proportional to a Laguerre polynomial L_n^m,

$$\hat{R}_n^{|m|} = \sqrt{\frac{2n!}{(n+|m|)!}} \lambda \rho^{|m|} \exp(-\tfrac{1}{2}\rho) L_n^{|m|}(\rho) \tag{9}$$

the adimensional variable ρ being defined as

$$\rho = \lambda R_c^2 \qquad \lambda = \frac{1}{\hbar}\sqrt{(A + 2C r_H^2) M}. \tag{10}$$

For a given set of parameters A, B and C, the potential V_M is determined and the numerical solution of the Schrödinger equation (6) provides the eigenvalues E_j and the set of corresponding coefficients $a_{nm\ell}^j$ appearing in the linear combination (7).

Table 1. Comparison between the methyl energy levels scheme worked out from the INS cross-section and the scheme resulting from the potential given by (3)–(5) with $A = -2.83$ meV Å^{-2}, $B = 0.39$ meV Å^{-4} and $C = 2.81$ meV Å^{-4}. Data are in meV units.

Level	Observed	Calculated	Obs. − calc.
I	0.626(1)	0.641	−0.015
II	1.849(5)	1.814	0.035
III	2.21(1)	2.276	−0.066
IV	2.48(1)	2.456	0.024
V	2.73(3)	2.803	−0.073

4. Interpretation of the experimental results

The scattering function $S(\boldsymbol{Q}, \omega)$ for the problem being considered is dominated by the spin-dependent contribution of the nuclear interaction between the neutron and the three protons. For unpolarized neutrons, $S(\boldsymbol{Q}, \omega)$ is given by [1]

$$S(\boldsymbol{Q}, \omega) \propto \sum_{i,f} p_i \sum_{s,s'} |\langle s'|\langle f|\hat{W}|i\rangle|s\rangle|^2 \delta(\hbar\omega + E_i - E_f). \tag{11}$$

Here $\boldsymbol{Q}$ is the neutron scattering vector, $\hbar\omega$ is the energy transfer, $|i\rangle$ is the initial molecular eigenstate with energy E_i and thermal occupation probability p_i, $|f\rangle$ is the final molecular state with energy E_f, $|s\rangle$ and $|s'\rangle$ are the initial and the final neutron spin state. The interaction operator W is given by

$$\hat{W} = \sum_{j=1}^{3} \boldsymbol{s} \cdot \boldsymbol{I}_j \exp(\mathrm{i}\boldsymbol{Q} \cdot \boldsymbol{r}_j) \tag{12}$$

where $\boldsymbol{s}$ is the neutron spin operator, whereas $\boldsymbol{I}_j$ and $\boldsymbol{r}_j$ are the spin and position operator for the jth proton. Equation (11) is valid if line broadening due to lifetime effects is negligible; it shows that the INS cross-section consists of a sequence of δ-functions, the positions of which are determined by the eigenvalues of the Schrödinger equation (6). Information on the eigenfunctions is obtained from the scattering intensities via the matrix elements of W. Averaged over all possible orientations of $\boldsymbol{Q}$, the $S(\boldsymbol{Q}, \omega)$ values given by (11) can be compared with the experimental results obtained for powder samples. The calculation of the cross-section (11) has been performed using the molecular wavefunctions given by (7), following the procedure developed in [16], where the intensities for transitions between librational levels of CH_3 and CH_4 molecules are evaluated.

To interpret the experiment, we supposed that the peaks in the INS cross-section shown in figure 2 correspond to transitions between different states of the p-xylene methyl groups. Energy and intensity of the methyl transitions were calculated for different choices of the model parameters, and the results allowed us to conclude that the energy level scheme compatible with the experimental observations is the one shown in figure 5. It must be noticed that this empirical level scheme is not compatible with the usual uniaxial rotor model for the CH_3 dynamics. Given the near free rotational value of the 0→I level, it cannot be reproduced by any combination of threefold plus sixfold potentials. Assuming the level scheme of figure 5, the final set of parameters $A = -2.83$ meV Å^{-2}, $B = 0.39$ meV Å^{-4} and $C = 2.81$ meV Å^{-4} was obtained by a best-fit procedure. The effective molecular potential for these parameters is ($B_M = 0.647$ meV)

$$V_M/B_M = 7.44R_c^2 + 3.26R_c^4 + 2.03R_c\cos(\Phi_c + 3\alpha) + 0.45R_c^4\cos(4\Phi_c). \tag{13}$$

The energy level scheme calculated with the potential (13) is compared with the experimental one in table 1. The composition of the molecular wavefunctions is given in table 2, and the comparison between observed and calculated intensities is given in table 3. As it can be seen, the model gives the correct values for the transition energies, but it also provides a good prediction of the transition intensities, although the value obtained for the last one is somewhat overestimated. The measurements were performed at fixed scattering angle, and there is a variation of Q with the energy transfer. This variation is, however, small in the energy range spanned (about 20%) and we have ignored the effects of the hydrogen zero-point vibrational Debye Waller factor.

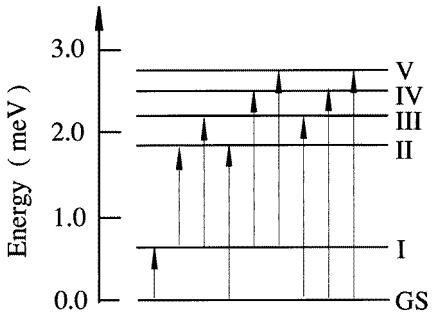

Figure 5. Energy level scheme for the rotation–translation motion of the *p*-xylene methyl groups in the calixarene complex. The arrows indicate transitions with non-zero intensity.

Table 2. Composition of the methyl roto-translational wavefunctions; the $|nm\ell\rangle$ kets are products of 2D oscillator and 1D rotator eigenstates. Only the three largest components are reported.

Ground state	$0.9973\|0, 0, 0\rangle + 0.0545\|1, 0, 0\rangle - 0.0333\|0, \pm1, \pm3\rangle$
I	$0.9960\|0, 0, \pm1\rangle - 0.0673\|0, \mp1, \mp2\rangle + 0.0530\|1, 0, \pm1\rangle$
II	$0.9904\|0, \pm1, 0\rangle + 0.1090\|1, \pm1, 0\rangle - 0.0650\|0, 0, \mp3\rangle$
III	$0.7816\|0, \pm1, \pm1\rangle - 0.6172\|0, 0, \mp2\rangle + 0.0846\|1, \pm1, \pm1\rangle$
IV	$0.9892\|0, \mp1, \pm1\rangle + 0.1072\|1, \mp1, \pm1\rangle - 0.0897\|0, \mp2, \mp2\rangle$
V	$0.7842\|0, 0, \mp2\rangle + 0.6104\|1, \pm1, \pm1\rangle + 0.0864\|1, 0, \mp2\rangle$

Table 3. Comparison between observed and calculated integrated intensities at $T = 4$ K. The values have been normalized to the intensity of the peak at 0.626 meV.

Transition	Energy (meV)	Obs. intensity	Calc. intensity
$0 \rightarrow$ I	0.626	100 ($\pm$3)	100
I $\rightarrow$ II	1.24	2 ($\pm$1)	2
I $\rightarrow$ III	1.60	11 ($\pm$3)	12
$0 \rightarrow$ II + I $\rightarrow$ IV	1.85	39 ($\pm$4)	39
I $\rightarrow$ V	2.10	15 ($\pm$1)	15
$0 \rightarrow$ III	2.21	19 ($\pm$2)	17
$0 \rightarrow$ IV	2.48	13 ($\pm$1)	12
$0 \rightarrow$ V	2.73	4 ($\pm$3)	12

The results obtained give evidence of the correctness of the roto-translation model proposed for the CH_3 dynamics in the investigated complex. We stress again that a test

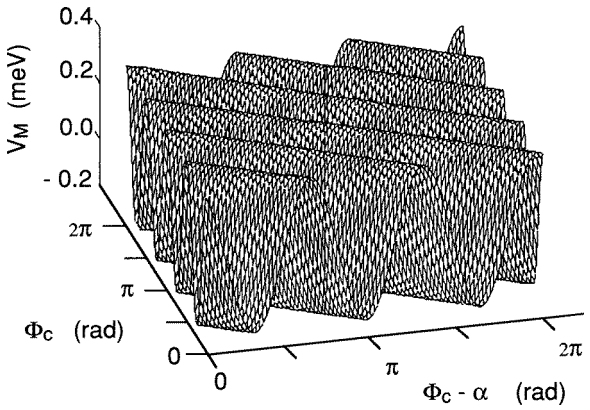

Figure 6. Effective molecular potential surface $V_M(R_c, \Phi_c, \alpha)$ for $R_c = 0.13$ Å, corresponding to the absolute minima. The coordinates of the valleys are related by $\Phi_c/3\alpha =$ constant.

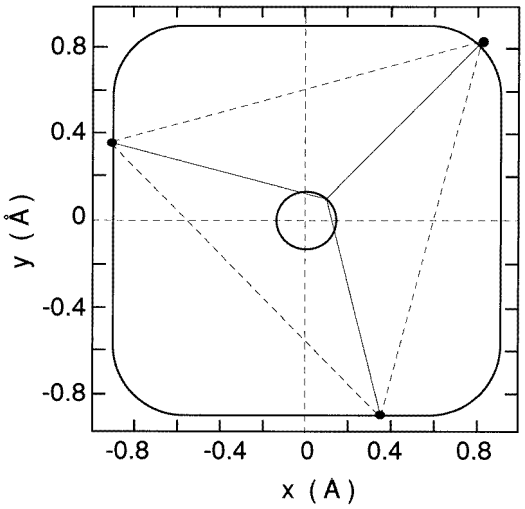

Figure 7. Classical orbit of the protons moving along a minimum valley of the effective molecular potential V_M. The circle is the loop described by the methyl centre of mass.

which is based not only on the comparison between eigenvalues and observed energies but also on the comparison between observed and calculated intensities is very stringent and, consequently, the proposed model can be deemed as physically sound.

The potential given by (13) is characterized by a harmonic term with strength $\lambda = 3.21$ meV Å^{-2}, an anharmonic contribution with intensity measured by $B + C = 3.2$ meV Å^{-4} and an anisotropic term with strength $B = 0.39$ meV Å^{-4}, measuring the coupling between the CM rotation and the re-orientation of the proton triangle. The absolute minima of this potential are found for $R_{cmin} = 0.13$ Å, at the angular positions given by $\Phi_c = \pm\pi/4, \pm 3\pi/4$ and $\alpha = \Phi_c + 2n\pi/3 (n = 0, 1, 2)$. The section of the potential surface at $R_c = R_{cmin}$ is drawn in figure 6 and shows the presence of steep hills, with flat valleys for angular parameters related by $\Phi_c/3\alpha =$ constant. For $R_c \neq R_{cmin}$ a very weak undulation appears owing to the $R_c^4 \cos(4\Phi_c)$ term. The molecular motion across

the minimum valleys corresponds to hypocycloidal orbits of the methyl protons, which are similar to the trajectory of a tooth of a three-toothed gear wheel in a fourfold gear rim. The proton orbits in the present case are shown in figure 7, together with the almost circular trajectory of the methyl centre of mass.

The wavefunctions reported in table 2 can be used to evaluate the density distribution of the methyl protons $\rho(\boldsymbol{r}, T)$ at a given temperature T, provided the T dependence of the potential may be neglected. The distributions obtained at $T = 4$ K and $T = 30$ K are shown in figure 8. High densities are, of course, found along the classical trajectories where the effective molecular potential is at a minimum. Experimental values of $\rho(\boldsymbol{r}, T)$ could be, in principle, determined by neutron diffraction on single crystals. Unfortunately, sufficiently large samples are not available at present, and it was not possible to verify the model predictions.

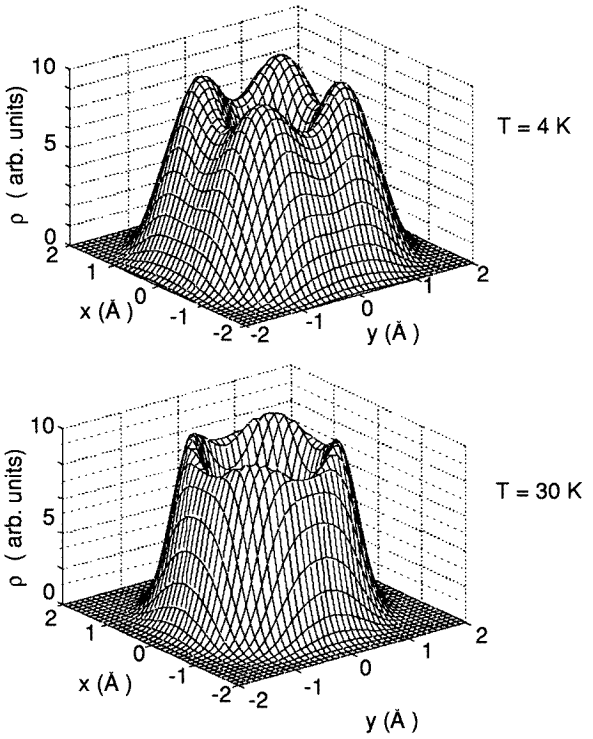

Figure 8. Proton density distribution in the plane of the CH_3 motion, calculated at $T = 4$ K and $T = 30$ K using the molecular wavefunctions obtained from the neutron spectroscopy investigation.

5. Conclusions

The rotational dynamics of the methyl groups in a quasi-free solid-state environment is often characterized by subtle coupling effects in virtue of which the unidimensional rotation single-particle model is inadequate to describe the results of spectroscopic measurements. The data interpretation in the framework of more sophisticated models is usually done only on the basis of measured frequencies; this is an unsatisfactory procedure because physically

different model Hamiltonians may have the same spectrum in the limited energy range which is scanned by the experiment. However, peak intensities also contain very useful information, allowing the test of eigenfunctions as well.

Here, we have presented an interpretation of the neutron spectroscopy results obtained for the methyl groups in a supramolecular complex characterized by a particularly weak host–guest interaction. We assume that CH_3 groups move in an effective anharmonic potential containing an anisotropic term which couples the uniaxial rotational motion of the proton triangle with the translational motion of its centre of mass, along a closed trajectory in a plane perpendicular to the rotation axis. Three parameters are sufficient to define the molecular potential up to the fourth order; they have been determined from the INS data by least-squares fitting, and by taking into account both energy and intensity of the observed excitations. The wavefunctions obtained from the solution of the corresponding Schrödinger equation have been used to predict the methyl proton density distribution which could be observed by neutron diffraction on single crystals.

Acknowledgments

The sample used in this investigation was kindly provided by Dr Franco Ugozzoli, of the University of Parma (Italy). We are indebted to Dr C J Carlile, ISIS facility, Rutherford Appleton Laboratory, for many useful discussions during the preparation of this work. We would also like to thank Dr David Martin for his collaboration in the preparation of the experiment at ISIS.

References

[1] Press W 1981 *Single Particle Rotations in Molecular Crystals (Springer Tracts in Modern Physics 92)* (Berlin: Springer)
[2] Carlile C J and Prager M 1993 *Int. J. Mod. Phys.* B **7** 3113
[3] Press W and Kollmar A 1975 *Solid State Commun.* **17** 405
[4] Cavagnat D, Lascombe J, Lassegues J C, Horsewill A J, Heidemann A and Suck J B 1984 *J. Physique* **45** 97
[5] Alefeld B, Kollmar A and Dasannacharja B A 1975 *J. Chem. Phys.* **63** 4415
[6] Caciuffo R, Amoretti G, Carlile C J, Fillaux F, Francescangeli O, Prager M and Ugozzoli F 1994 *Physica* B **202** 279
[7] Caciuffo R, Amoretti G, Carlile C J, Ferrero C, Geremia S, Paci B, Prager M and Ugozoli F 1997 *Physica* B **234–236** 115
[8] Fillaux F and Carlile C J 1990 *Phys. Rev.* B **42** 5990
[9] Heidemann A, Friedrich H, Günther E and Häusler W 1989 *Z. Phys.* B **76** 335
[10] Prager M, Caciuffo R, Amoretti G, Carlile C J, Coddens G, Fillaux F, Francescangeli O and Ugozzoli F 1994 *Mol. Phys.* **81** 609
[11] Diamond D and McKervey M A 1996 *Chem. Soc. Rev.* **25** 15 and references therein
[12] Andreetti G D and Ugozzoli F 1990 *Calixarenes* ed J Vicens and V Böhmer (Dordrecht: Kluwer)
[13] Caciuffo R, Amoretti G, Fillaux F, Francescangeli O, Melone S, Prager M and Ugozzoli F 1993 *Chem. Phys. Lett.* **201** 427
[14] Schiebel P, Hoser A, Prandl W, Heger G, Paulus W and Schweiss P 1994 *J. Phys.: Condens. Matter* **6** 10 989
[15] Havighorst M and Prager M 1996 *Chem. Phys. Lett.* **250** 232
[16] Matuschek D W and Hüller A 1988 *Can. J. Chem.* **66** 495